Gas-Phase Hydroformylation of Propene over Silica-Supported PPh$_3$-Modified Rhodium Catalysts

Taejin Kim · Fuat E. Celik · David G. Hanna · S. Shylesh · Sebastian Werner · Alexis T. Bell

Abstract Heterogeneous rhodium catalysts supported on SiO$_2$ were modified with PPh$_3$ for the gas-phase hydroformylation of propene to produce *n*- and isobutanal. High selectivity to aldehydes was achieved, with no propane or alcohols formed. Investigation of the effects of reaction temperature, reactant partial pressures, total pressure, and PPh$_3$/Rh ratio suggested that the supported catalyst behaved similarly to the homogeneous catalyst. In particular, the supported catalyst showed similar activation energies and partial and total pressure dependences of the reaction rates to those observed in homogeneous, liquid-phase reactions. The first order dependence of the hydroformylation rate on the partial pressures of propene, CO, and H$_2$ individually led to a cubic dependence of butanal formation on total pressure for equimolar reactant mixtures. High regioselectivity with a typical *n/i* ratio of 14 was achieved.

T. Kim · F. E. Celik · D. G. Hanna · S. Shylesh · S. Werner · A. T. Bell (✉)
Department of Chemical Engineering, University of California, Berkeley, Berkeley, CA 94720, USA
e-mail: bell@cchem.berkeley.edu

S. Werner
Friedrich-Alexander Universität Erlangen-Nürnberg, Lehrstuhl für Chemische Reaktionstechnik, Egerlandstraße 3, 91058 Erlangen, Germany

1 Introduction

Aldehydes are produced industrially by hydroformylation of olefins with synthesis gas. Homogeneous complexes of Rh and Co are the preferred catalysts for this process because of their high activity and tunable regioselectivity [1]. Since separating the products from the catalyst is often difficult, there has been an interest in identifying heterogeneous hydroformylation catalysts. While Rh-substituted X and Y zeolites have been reported to promote the hydroformylation of ethene and propene at atmospheric pressure [2, 3], they exhibit poor regioselectivity resulting in low molar normal/isoaldehyde (*n/i*) ratios of ∼2, and the olefin hydrogenation activity of these catalysts is comparable to that for hydroformylation. Hydroformylation of propene on silica-supported Rh, Pd, Pt, and Ni with and without promotion with Na has also been reported [4]. Na-promoted Pt/SiO$_2$ and Rh/SiO$_2$ exhibit the highest hydroformylation activities, but the rates of propene hydrogenation to propane are more than ten times higher. Similar results have been reported for Rh/SiO$_2$ and sulfur-promoted Rh/SiO$_2$ [5, 6]. Sulfur promotion enhances the rate of propene hydroformylation relative to the rate of propene hydrogenation, particularly at high pressure, but the selectivity to butanal is less than ∼30% at 10 atm. More recently, Ding and coworkers [7–12] have demonstrated that high activity, near 100% selectivity, and good stability for the hydroformylation of propene to butanal can be achieved with PPh$_3$-modified Rh/SiO$_2$. Characterization of these catalysts by ^{1}H, ^{29}Si, ^{31}P, and ^{17}O MAS NMR, suggests that the active species consist of Rh$^+$ species bound to the support via Si–O–Rh bonds, whereas IR spectra of the catalyst exposed to CO suggest that species similar to the homogeneous complex HRh(CO)$_2$(PPh$_3$)$_2$ are formed in situ on the surface of the catalyst. TEM images

taken of spent catalyst revealed the presence Rh nanoparticles ~ 1 nm in diameter, suggesting that the active catalyst contains metallic Rh as well as Rh^+ species. The coexistence of Rh^0 and Rh^+ was confirmed by XPS.

The present work was undertaken to investigate the effects of catalyst composition and reaction conditions on the kinetics of propene hydroformylation on a PPh₃-modified Rh supported on SiO_2 (PPh₃–Rh/SiO_2) catalyst. The effects of reaction temperature, total pressure, reactant partial pressure, and PPh₃/Rh ratio on the activity and selectivity of the catalysts were investigated. The results obtained were then compared to those obtained for Rh-based homogeneous hydroformylation catalysts.

2 Experimental

The preparation of PPh₃–Rh/SiO_2 catalysts followed previously described techniques [7–12]. 1 wt% Rh/SiO_2 was prepared by incipient wetness impregnation of mesoporous SiO_2 (Silicycle, 500 m² g⁻¹, average pore diameter 60 Å) with a solution of rhodium (III) acetylacetonate (Aldrich, 97% pure) dissolved in toluene (Alfa Aesar, anhydrous 99.8% pure). After impregnation, the solid was dried at 393 K for 12 h, then calcined in 100 cm³ min⁻¹ of 10% O_2/He (Praxair, certified standard) for 4 h at 673 K (2 K min⁻¹), and finally reduced in 100 cm³ min⁻¹ of 9% H_2/He (Praxair, certified standard) at 673 K for 4 h. Using incipient wetness impregnation, a solution of PPh₃ (Aldrich, 99% purity) in toluene was absorbed onto the SiO_2-supported Rh under a N_2 environment. After the impregnation, the solid was dried for 2 h at ambient temperature in an N_2 environment and then further dried in a vacuum oven at 338 K for 12 h. The PPh₃/toluene solution concentration was varied to give final molar ratios of PPh₃/Rh between 5 and 30. Most experiments were carried out with a PPh₃/Rh ratio of 15.

Rate measurements were carried out in a 6.35 mm OD quartz tube with an expanded section (~ 12.7 mm OD, ~ 20 mm length). The reactor was packed with quartz wool above and below the catalyst bed to hold the catalyst powder in place. The reactor was placed inside a resistively heated ceramic furnace with external temperature control and the catalyst bed temperature was measured with a K-type thermocouple sheathed in a quartz capillary placed in direct contact with the bed.

Prior to reaction, the catalysts was reduced by heating to 393 K for 2 h at the rate of 2 K/min in pure hydrogen (Praxair) flowing at 20 cm³ min⁻¹. The feed to the reactor consisted of propene (Praxair, 3.0 grade), CO (Praxair, 4.0 research grade), H_2 (Praxair, 5.0 UHP grade). A reactant ratio of C_3H_6:CO:H_2 of 1:1:1 was used unless specified otherwise. Experiments were carried out at total gas

pressures of 1–2.8 atm by throttling a needle valve located downstream from the reactor. Total gas flow rate was varied from 60–168 cm³ min⁻¹ at STP in order to maintain a constant volumetric flow rate of 60 cm³ min⁻¹ at pressure. Using these conditions, the conversion of propene was always less than 3%, indicating that the reactor operated under conditions of differential conversion.

Reaction products were analyzed using an Agilent 6890 N gas chromatograph containing a bonded polystyrene-divinylbenzene (HP-PLOT Q) capillary column connected to a flame ionization detector and a divinylbenzene (HayeSep DB) packed column connected to a thermal conductivity detector.

Transmission electron microscopy micrographs of the catalyst were obtained using a FEI Tecnai 12 TEM instrument operated at an accelerating voltage of 120 kV. TEM samples were prepared by dispersing the catalyst (0.01 g) in ethanol (2 mL) and sonicating for 5 min. Afterwards, a drop of the homogeneous suspension containing the catalyst was put over a Lacey carbon grid followed by the evaporation of the solvent under ambient conditions.

Infrared spectra were acquired using a Thermo Scientific Nicolet 6700 FTIR spectrometer equipped with a liquid nitrogen cooled MCT detector. Each spectrum was obtained by averaging 32 scans taken with 1 cm⁻¹ resolution. 0.015 g of PPh₃–Rh/SiO_2 was mixed with an equal mass of bare SiO_2 and pressed into a 20 mm-diameter pellet (<1 mm thick) and placed into a custom-built transmission cell equipped with CaF_2 windows, a K-type thermocouple for temperature control, and resistive cartridge heaters similar to that described in [13]. The sample was diluted with silica due to the high IR absorbance of the PPh₃ in the catalyst pores. All scans were acquired at 393 K. Experiments at elevated pressure were carried out by throttling a needle valve located downstream from the reactor. Pure CO was passed through a trap packed with 3.2 mm pellets of 3A molecular sieve in order to remove iron pentacarbonyl formed within the cylinder [14]. All absorption spectra were taken relative to the empty transmission cell. The spectrum of the catalyst under He flow was subtracted from all the results reported.

Solid-state ³¹P MAS NMR experiments were performed on a Bruker Avance I-500 MHz spectrometer. Data were obtained by measuring the samples using a frequency of 202.5 MHz, 90° pulse in 4.2 μs, and a delay of 60 s.

3 Results and Discussion

3.1 Catalytic Activity of PPh₃–Rh/SiO_2

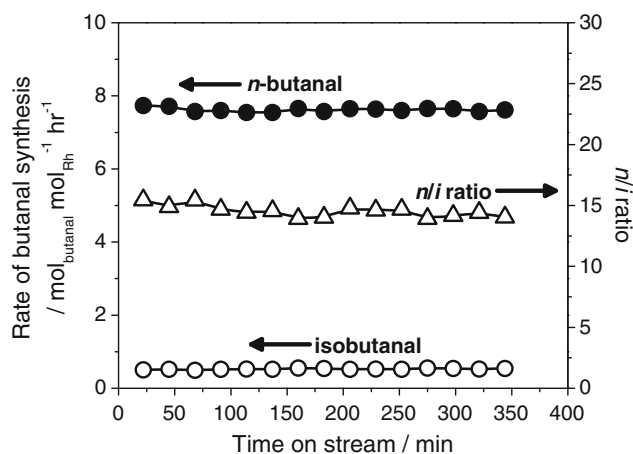To investigate the stability of the PPh₃-modified silica-supported Rh catalysts, 0.6 g of catalyst with PPh₃/

Fig. 1 The effect of time on stream on the rates of butanal synthesis. $P_{Total} = 2$ atm, $P_{C3H6}:P_{CO}:P_{H2} = 1:1:1$, $T = 393$ K, catalyst mass = 0.6 g, total gas flow rate = 60 cm^3 min^{-1} at pressure, 120 cm^3 min^{-1} at STP

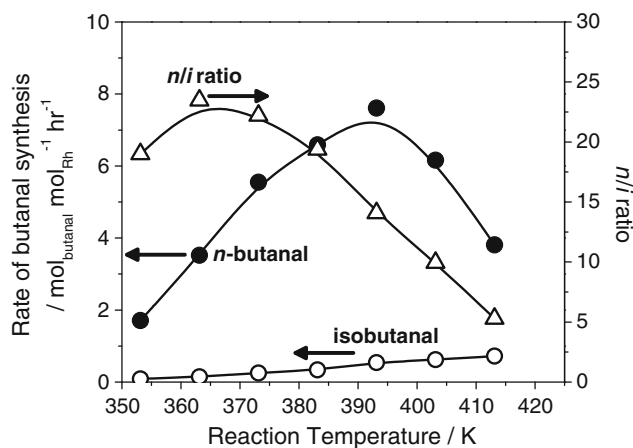

Fig. 2 The effect of reaction temperature on the rates of butanal synthesis. $P_{Total} = 2$ atm, $P_{C3H6}:P_{CO}:P_{H2} = 1:1:1$, catalyst mass = 0.6 g, total gas flow rate = 60 cm^3 min^{-1} at pressure, 120 cm^3 min^{-1} at STP

Fig. 3 Activation energies of n-/isobutanal formation. $P_{Total} = 2$ atm, $P_{C3H6}:P_{CO}:P_{H2} = 1:1:1$, catalyst mass = 0.6 g, total gas flow rate = 60 cm^3 min^{-1} at pressure, 120 cm^3 min^{-1} at STP. Rate of butanal synthesis is plotted on a logarithmic scale

Rh = 15 was contacted with an equimolar gas mixture of propene, CO, and H$_2$ at 393 K for ~6 h, as shown in Fig. 1. During this time, the activity of the catalyst for hydroformylation was constant, after an initial transient period during the first ~20 min. The selectivity to aldehydes was 100% and the molar n/i ratio remained constant at ~14. Neither propane nor butanol was observed in the reactions products.

The effect of reaction temperature on the rates of n- and isobutanal synthesis and the molar n/i ratio are shown in Fig. 2. The rate of n-butanal formation increased with temperature up to 393 K, after which it decreased. The rate of isobutanal formation showed much less sensitivity to temperature over the range investigated. The selectivity to aldehydes was 100% for temperatures of 353–413 K. The
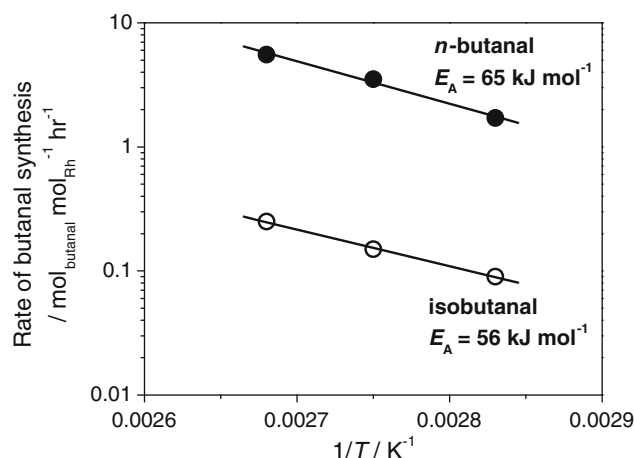
ratio of n- to isobutanal reached a maximum value of 21 at 363 K and then decreased to 5 at 413 K. Figure 3 shows an Arrhenius plot of the reaction rate with temperature in the range 353–373 K from which the activation energy for propene hydroformylation to n-butanal and isobutanal were calculated as 65 and 56 kJ/mol, respectively.

Figure 4 shows the effect on total reaction pressure on the rate of propene hydroformylation for equimolar reaction mixtures of C$_3$H$_6$, CO, and H$_2$ at 393 K. Increasing the total pressure up to 2.8 atm increased the rate of formation of both n-butanal and isobutanal. By plotting reaction rates on a log–log plot and taking the slope of the date, the inset of Fig. 4 shows that the dependences of n- and isobutanal formation rates on total pressure were 3.13 and 2.89, respectively.

To measure the dependences of the butanal formation rates on the individual partial pressures of propene, CO, and H$_2$, two component partial pressures were fixed at 0.67 atm while the partial pressures of the third reactant and that of He were varied. The total gas flow rate and pressure were kept constant at 60 cm^3 min^{-1} and 2 atm (120 cm^3 min^{-1} at STP). Figure 5a–c show the effects of varying the partial pressures of C$_3$H$_6$, CO, and H$_2$ partial pressures. While the dependence of the formation rates for the two butanal isomers on C$_3$H$_6$ partial pressure were nearly equal (1.01 and 0.99 for n- and isobutanal), the dependences on CO and H$_2$ partial pressures were greater for the linear product (1.12 and 1.02) as compared to the branched product (0.90 and 0.85), leading to higher n/i ratios at higher CO and H$_2$ partial pressures.

Summing the partial pressure dependences of the n-butanal formation rate on the individual reactants from Fig. 5 gives a 3.15 dependence on total pressure for equimolar reactant mixtures, in good agreement with the value
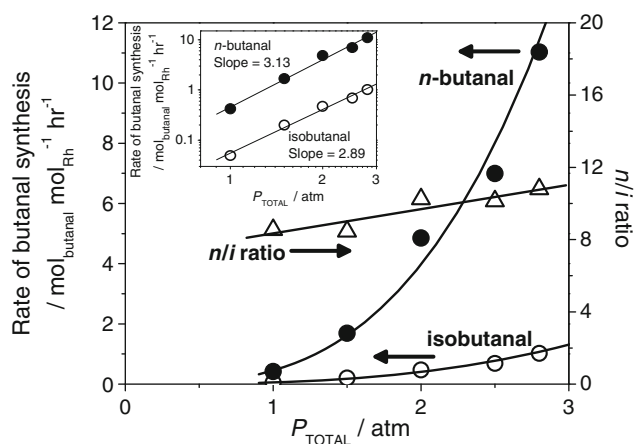
Fig. 4 The effect of total pressure on the rates of butanal synthesis. $P_{Total} = 1$–2.8 atm, $P_{C3H6}:P_{CO}:P_{H2} = 1:1:1$, $T = 393$ K, catalyst mass = 0.15 g, total gas flow rate = 60 cm^3 min^{-1} at pressure, 60–168 cm^3 min^{-1} at STP. *Inset*: rate of butanal synthesis as a function of total pressure in a log–log plot

of 3.13 obtained from the total pressure dependence derived from Fig. 4. The same calculation for isobutanal sums to 2.74, compared with 2.89 obtained from Fig. 4.

The role of the PPh$_3$ on the performance of the catalyst was investigated by varying the molar ratio of the ligand to the Rh. Figure 6 shows the effects of the bulk PPh$_3$/Rh ratio on activity and n/i ratio. In the absence of PPh$_3$, Rh/SiO$_2$ is inactive for hydroformylation. The hydroformylation activity for both n-butanal and isobutanal formation increased rapidly with increasing PPh$_3$/Rh ratio up to a ratio of 15. Above this value, the activity towards both products declined rapidly, giving rise to a sharp maximum at a PPh$_3$/Rh of 15. The rate of linear product formation grew faster than the branched product, even up to a PPh$_3$/Rh ratio of 20, increasing the n/i ratio from ~ 4 to ~ 15. From a PPh$_3$/Rh ratio of 20 to 30, the rate of n-butanal formation decreased more rapidly than the rate of isobutanal formation, leading to an n/i ratio ~ 10.
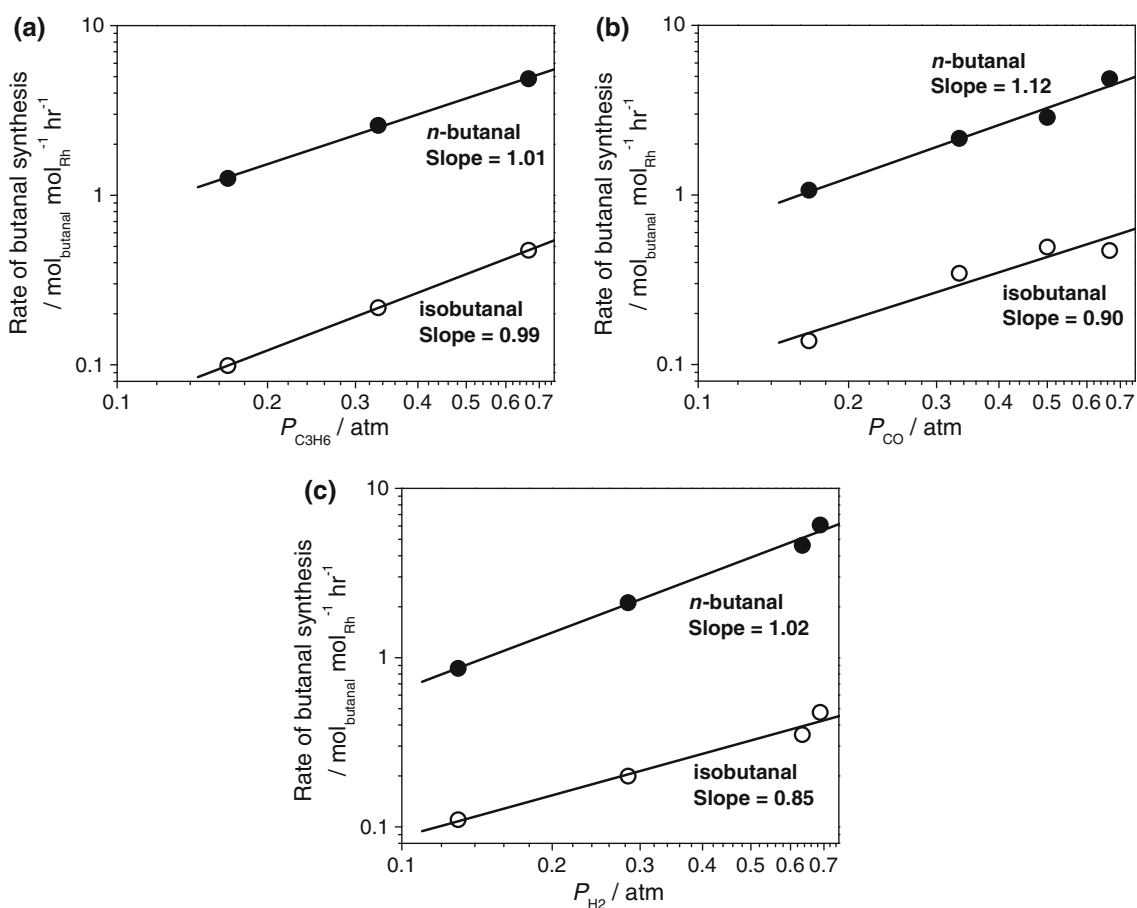

Fig. 5 The effect of propene, CO, and H$_2$ partial pressures on the rates of butanal synthesis; (**a**) P_{C3H6}, (**b**) P_{CO}, (**c**) P_{H2}. $P_{Total} = 2$ atm, catalyst mass = 0.6 g, total gas flow rate = 60 cm^3 min^{-1} at pressure, 120 cm^3 min^{-1} at STP. **a** $P_{CO} = P_{H2} = 0.67$ atm, balance He, (**b**) $P_{C3H6} = P_{H2} = 0.67$ atm, balance He, (**c**) $P_{C3H6} = P_{CO} = 0.33$ atm, balance He. Rate of butanal synthesis and reactant partial pressures plotted on logarithmic scales

The dependence of the *n/i* ratio on PPh$_3$ concentration and total pressure can be attributed to the equilibrium shown in Scheme 1 [15]. HRh(CO)$_4$ forms in the absence of PPh$_3$ and/or at very high CO pressures. This species, if formed, would possess a higher activity but yield a lower *n/i* ratio as compared to other HRh(CO)$_n$(PPh$_3$)$_{4-n}$ species [16]. In the presence of PPh$_3$, HRh(CO)$_n$(PPh$_3$)$_{4-n}$ species with *n* = 1–3 may form. These 18 e$^-$ species must lose a ligand in order to form the coordinatively unsaturated 16 e$^-$ HRh(CO)$_m$(PPh$_3$)$_{3-m}$ species, which are the active intermediates. In Fig. 6, almost no reaction is seen when PPh$_3$ is absent because HRh(CO)$_4$ formation is disfavored at the low CO partial pressures used. As the ligand concentration increases, the equilibria in Scheme 1 shift to the left, the steric bulk of the complexes in solution increases which results in higher *n/i* ratios. When the concentration of PPh$_3$ is increased, it becomes more difficult for the 18 e$^-$ complexes to lose a PPh$_3$ ligand and form the 16 e$^-$ species. This leads to a decrease in activity. The decrease in the *n/i* ratio at higher PPh$_3$:Rh ratios arises from the activity of *n* = 2 and *n* = 3 species that can form the 16 e$^-$ intermediates through CO loss, whereas *n* = 1 cannot. Hence, the complex with the highest regioselectivity for the linear product becomes inactive relative to the other complexes at high ligand concentrations.

The hydroformylation activity of the PPh$_3$–Rh/SiO$_2$ catalyst prepared in this study is compared in Table 1 with those for similar catalysts prepared in which SiO$_2$, MCF, and SBA-15 were used as supports [8, 9, 11, 17]. Also shown are the results for SiO$_2$- and SBA-15-supported solutions of HRh(CO)(PPh$_3$)$_3$ in PPh$_3$ [8, 11]. In all cases, except where sulfoxantphos was used, the PPh$_3$/Rh ratio was 15. Since the studies reported in [8, 9, 11, 15] were done at 10 atm, we have used the observed dependence on
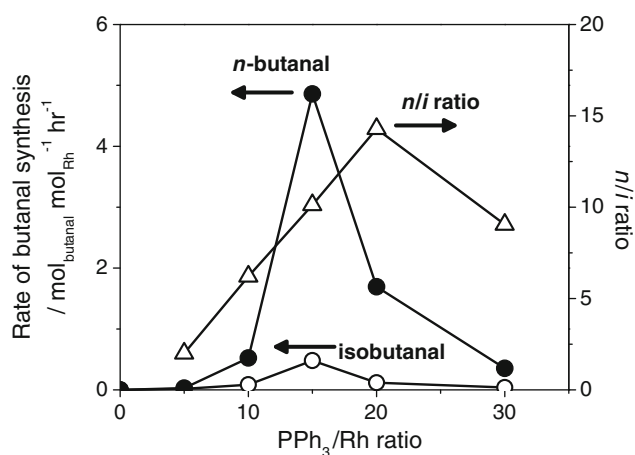

Fig. 6 The effect of PPh$_3$/Rh ratio on the rates of butanal synthesis. P_{Total} = 2 atm, P_{C3H6}:P_{CO}:P_{H2} = 1:1:1, *T* = 393 K, catalyst mass = 0.15 g, PPh$_3$/Rh molar ratio = 0–30, total gas flow rate = 60 cm^3 min^{-1} at pressure, 120 cm^3 min^{-1} at STP
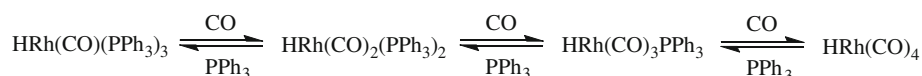
total pressure for equimolar reactant mixtures, 3.1, to adjust the rate of butanal formation that we observe at a total pressure of 2.8 atm up to a total pressure of 10 atm. It is evident that the projected activity for our PPh$_3$–Rh/SiO$_2$ catalyst is similar to those reported by Ding and co-workers.

The activation energies measured in this study for the formation of *n*- and isobutanal are compared in Table 2 with those reported for Rh(CO)$_2$(acac) dissolved in 2,2,4-trimethyl-1,3-pentanediol containing PPh$_3$ in an amount corresponding to PPh$_3$/Rh ~ 19 [18], as well as for supported Rh catalysts [15, 19]. The activation energies for both isomers of butanal observed for the heterogeneous and homogeneous systems are remarkably similar. It is also notable that the rates of formation of both butanal isomers are reported to be first order in all three reactants, C$_3$H$_6$, CO, and H$_2$, for the homogenously catalyzed reaction [20] in close agreement with the observations of the present study. These strong similarities between the kinetics parameters for the heterogeneous and homogeneously catalyzed hydroformylation of propene suggest that a homogeneous catalyst of the type HRh(CO)$_n$(PPh$_3$)$_{4-n}$ is produced when PPh$_3$–Rh/SiO$_2$ is exposed to reaction conditions. This proposal is consistent with that made in earlier studies of PPh$_3$–Rh/SiO$_2$ catalysts [7–12] and is further supported by physical characterization described next.

3.2 Catalyst Characterization

Figure 7 shows a TEM image of the as-prepared Rh/SiO$_2$ catalyst. Particles of Rh with diameters of 1–2 nm are evident. The IR spectrum of this sample of Rh/SiO$_2$ exposed to 0.2–1.0 atm of CO at 393 K exhibited a strong band at 2060 cm^{-1} and a broad band at 1880 cm^{-1}. In addition, a distinct peak shoulder was observed at 2084 cm^{-1}, and another peak shoulder was observed on the low-energy side of the peak at 2060 cm^{-1}. The peaks at 2060 and 1880 cm^{-1} arise due to CO linearly adsorbed on the Rh nanoparticles, and CO bridge-bonded on the Rh nanoparticles respectively [21, 22]. The shoulder at 2084 cm^{-1} can be attributed to asymmetric C–O stretching vibrations of Rh(I)(CO)$_2$ species formed by reaction of the Rh nanoparticles with CO and Si–OH groups of the support [19, 20], while the lower energy shoulder arises from the symmetric C–O stretch of these Rh(CO)$_2$ species.

Figure 8 shows IR spectra obtained when Rh/SiO$_2$ impregnated with PPh$_3$ (PPh$_3$/Rh = 15) was exposed to increasing pressures of CO at 393 K. The sharp peaks above 2000 cm^{-1} appearing in each spectrum are due to the rovibrational R-bands of gaseous CO. For very low CO partial pressure (0.02 atm) a broad band at ~2016 cm^{-1} and a somewhat better defined band centered at 1970 cm^{-1} were observed. The intensity of these bands did not change

$$HRh(CO)(PPh_3)_3 \underset{PPh_3}{\overset{CO}{\rightleftharpoons}} HRh(CO)_2(PPh_3)_2 \underset{PPh_3}{\overset{CO}{\rightleftharpoons}} HRh(CO)_3PPh_3 \underset{PPh_3}{\overset{CO}{\rightleftharpoons}} HRh(CO)_4$$

Scheme 1 Equilibrium of rhodium catalysts containing phosphorus and carbonyl ligands

Table 1 Comparison of hydroformylation activity for different supported Rh catalysts

Catalyst	Activity (h^{-1})	Pressure (atm)	Temperature (K)	Reference
PPh$_3$–Rh/SiO$_2$	340	10[a]	393	This work
HRh(CO)(PPh$_3$)$_3$/SiO$_2$	230	10	393	[8]
HRh(CO)(PPh$_3$)$_3$/SBA-15	301	10	393	[11]
PPh$_3$–Rh/SiO$_2$	131	10	393	[8]
PPh$_3$–Rh/MCF	161	10	393	[9]
PPh$_3$–Rh/SBA-15	245	10	393	[11]
HRh(CO)$_2$–Sulfoxantphos/SiO$_2$	381	10	393	[17]

[a] Results from this work taken at lower pressure were scaled to 10 atm using a 3.1 dependence on total pressure for equimolar reactant mixtures

Table 2 Comparison of activation energies for the formation of n- and isobutanal

Catalyst	Reaction Phase	E_A (kJ/mol)	Pressure (atm)	Temperature (K)	Reference
PPh$_3$–Rh/SiO$_2$	Gas	65.0[a]	2	353–373	This work
		57.0[b]			
Rh/PPh$_3$	Liquid	68.1[a]	10	358–388	[18]
		58.0[b]			
HRh(CO)$_2$–Sulfoxantphos/SiO$_2$	Gas	63.3[a]	12	338–417	[17]
HRh(CO)(PPh$_3$)$_3$/Al$_2$O$_3$	Liquid	70.6[a]	16	363–383	[19]

[a] n-butanal

[b] isobutanal

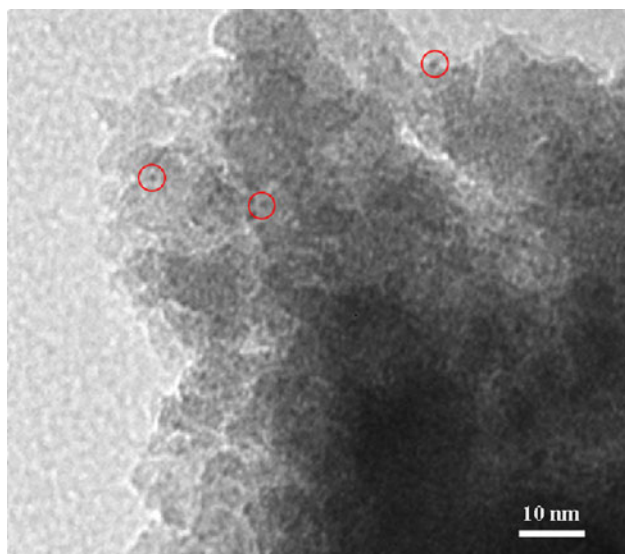**Fig. 7** TEM micrograph of PPh$_3$–Rh/SiO$_2$ catalyst before exposure to reactant gases. Rh nanoparticles (examples highlighted within *red circles*) can be seen

further upon increasing the CO partial pressure. The assignment of these bands is uncertain, but the broad peak at 2016 cm^{-1} probably arises from the linear Rh(CO) species red-shifted due to the presence of PPh$_3$ and residual moisture [11, 19]. The band at 1970 cm^{-1} is best assigned to vibrations of a CO molecule that bridges between to Rh(I) cations that interact with the support via Rh–O–Si bonds, and which may have linearly bound CO molecules associated with one or both Rh cations [23]. As the CO partial pressure was increased, two new bands appeared at 1999 and 1939 cm^{-1}, which grew with nearly constant relative intensities. These peaks agree well with previous reports of HRh(CO)(PPh$_3$)$_3$ and HRh(CO)$_2$(PPh$_3$)$_2$ species sorbed into porous supports [7, 11, 24], homogeneous liquid-phase spectra of HRh(CO)$_n$(PPh$_3$)$_{4-n}$ species [25–27], and reports of PPh$_3$–Rh/SiO$_2$ catalysts following CO exposure [8, 11]. The band at 1999 cm^{-1} arises due to an intense C–O vibration of HRh(CO)(PPh$_3$)$_3$ and the band at 1939 is due to a similar vibration in HRh(CO)$_2$(PPh$_3$)$_2$. The weaker C–O vibrational modes of these species were likely

obscured by the other peaks of the spectra between 1900 and 2050 cm^{-1}. At higher CO partial pressures (i.e., 2.0 and 3.0 atm), a new band appeared at 2066 cm^{-1} (Fig. 8, inset). This band can be assigned to the asymmetric C–O stretch of geminal dicarbonyl $Rh(CO)_2$ species, shifted to lower energy by the presence of PPh_3 and moisture[11, 19]. The symmetric stretch is likely obscured by other, more intense, bands.

The growth of bands associated with $HRh(CO)(PPh_3)_3$ and $HRh(CO)_2(PPh_3)_2$ with increasing CO partial pressure provides strong additional evidence for the in situ formation of homogeneous, Wilkinson-type catalysts. The nearly linear growth of these bands with increasing CO pressure implies that an equilibrium exists between gaseous CO, Rh metal, and homogeneous $HRh(CO)_n(PPh_3)_{4-n}$ species.

Further evidence for the formation of homogenously dispersed Rh under reaction conditions was obtained from ^{31}P NMR spectroscopy. Figure 9 shows the results of solid-state ^{31}P MAS NMR measurements of (a) phosphine modified silica (PPh_3–SiO_2), (b) freshly prepared PPh_3–Rh/SiO_2, and (c) spent PPh_3–Rh/SiO_2. The sharp peak observed at −5.6 ppm for PPh_3/SiO_2 sample can be ascribed to the free PPh_3 adsorbed on the silica surface [11, 12]. The PPh_3–Rh/SiO_2 sample showed the presence of free phosphine at −5.6 ppm and a less intense, broad peak centered at 32.5 ppm due to the phosphine chemisorbed over the rhodium nanoparticles [12]. However, the spent PPh_3–Rh/SiO_2 catalyst showed a sharp peak at 29.7 ppm. This band is not
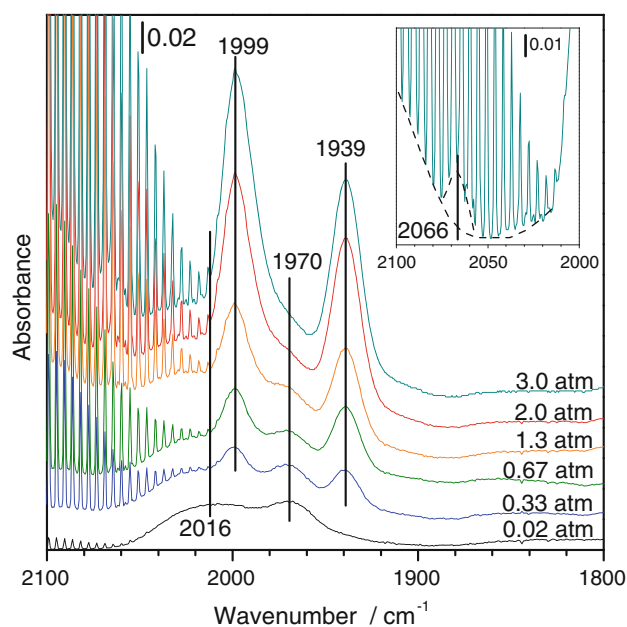
due to free $HRh(CO)(PPh_3)_3$, which exhibits peaks at 34.4 and 45.4 ppm [28]. However, it has been observed that when supported on MCM-41 or MCM-48, the ^{31}P resonance of $HRh(CO)(PPh_3)_3$ broadens and shifts to 25.4 and 26.0 ppm, suggesting some interaction between the complex and the support [25]. A peak at 28.9 ppm has also been reported in a study of PPh_3–Rh/SBA-15 after use of this material for the hydroformylation of propene, which is assigned by the authors to a Rh-phosphine complex [12]. Therefore, while the peak at 29.7 ppm, shown in spectrum (c) of Fig. 9 cannot be assigned definitively, it is very like due to some form of homogeneously dispersed Rh possessing both CO and PPh_3 ligands.

3.3 Kinetics of Propene Hydroformylation

The observed kinetics of butanal formation are rationalized based on the mechanism shown in Scheme 2 derived from solution chemistry. Since there is no definitive evidence for interactions between the support surface and the active catalytic species, we envision a Rh species dissolved in molten PPh_3 (melting point of PPh_3 is 80 °C) yielding $HRh(CO)_n(PPh_3)_{4-n}$ as the catalyst. As further support for the assumption that hydrofomylation only involves homogeneous species, we note that the kinetics reported here are comparable to those reported for propene hydroformylation carried out in homogeneous solutions.

$HRh(CO)(PPh_3)_3$ (**A**) and $HRh(CO)_2(PPh_3)_2$ (**B**) are present in equilibrium with each other (Reaction 1) and that hydroformylation of propene is initiated by the loss of a CO ligand to form the 16-electron species, $HRh(CO)(PPh_3)_2$ (**C**) via Reaction 2. Propene coordinates with the latter species via Reaction 3 to form species **D** after which this species undergoes migratory insertion into the Rh–H bond to form a propyl species (**E**) via Reaction 4. CO then
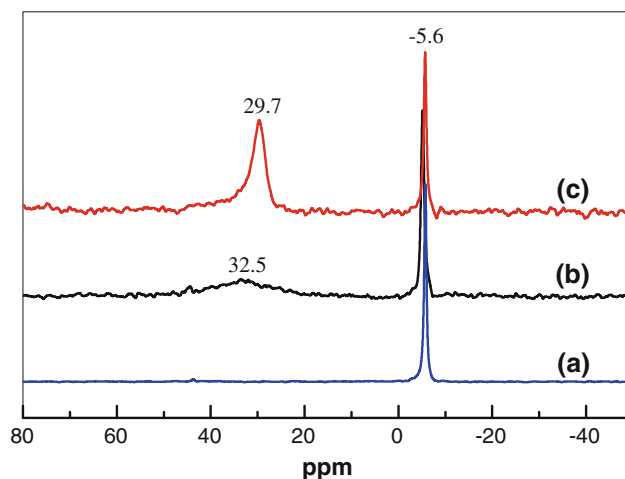

Fig. 8 FTIR spectra of PPh_3–Rh/SiO_2 under CO flow at different partial pressures, as indicated in the figure. The *inset* shows an additional band observed at higher CO partial pressures (e.g. 3.0 atm) partially obscured by the rovibrational vibrations for the R-branch of gaseous CO

Fig. 9 Solid-state ^{31}P MAS NMR spectra of (*a*) PPh_3/SiO_2, (*b*) PPh_3–Rh/SiO_2 and (*c*) spent PPh_3–Rh/SiO_2 catalyst
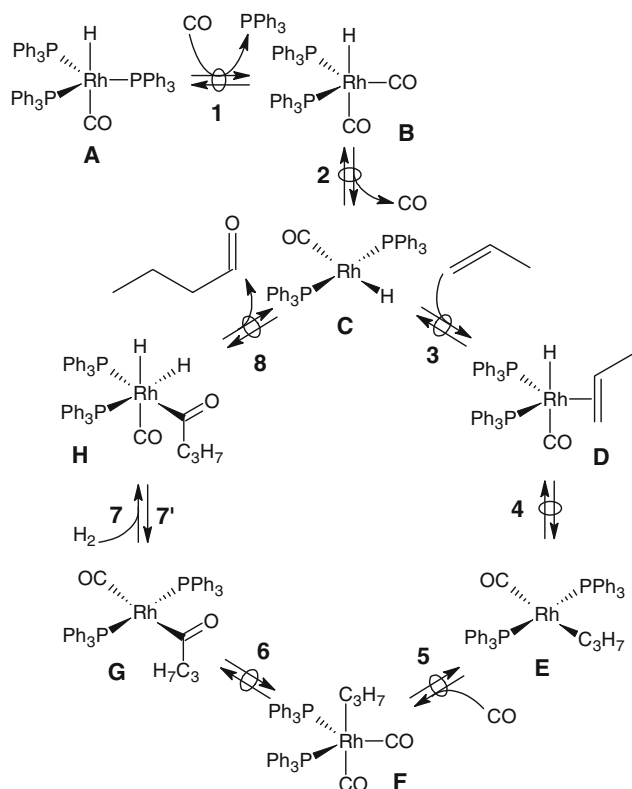
Scheme 2 Proposed mechanism for the homogeneous hydroformylation of propene

adds to species **E** to form an 18-electron intermediate (**F**) in Reaction 5. Migratory insertion of the propyl to a carbonyl group leads to the formation of an acyl intermediate (**G**) via Reaction 6. Oxidative addition of H_2 (Reaction 7) forms the 18-electron Rh(III) species (**H**) in the rate-limiting step, followed by the reductive elimination of butanal (Reaction 8) returning to species **C**. The 18-electron species **A** and **B** are thought to be the most abundant species in solution under reaction conditions. It should be noted that mechanism shown in Scheme 2 focuses on the formation of n-butanal, the dominant product observed in all cases, and that no attempt was made to develop a similar scheme for iso-butanal, since it is not clear which Rh species are responsible for forming this product.

If it is assumed that Reactions 1–6 and Reaction 8 are at quasi-equilibrium and that Reaction 7 is the rate-limiting step and is irreversible, then it can be shown that the rate of butanal formation will be given by the following relation:

$$r_{n-\text{butanal}} = \frac{k_7 \prod\limits_{i=1}^{6} K_i P_{C_3H_6} P_{CO} P_{H_2}/[PPh_3]}{(1 + K_1 P_{CO}/[PPh_3])}[Rh]_0 \quad (1)$$

Here k_7 is the rate coefficient for Reaction 7, K_i is the equilibrium constant for Reaction i, P_j is the partial pressure of species j, and [PPh$_3$] is the concentration of species

PPh$_3$, and [Rh]$_0$ is the total concentration of Rh in solution. If it is further assumed that the second term in the denominator of Eq. 1 is small relative to unity, then the form of the rate expression is consistent with the observed kinetics for condition where the ratio of PPh$_3$ to Rh is large, i.e. [PPh$_3$]/[Rh] > 10.

It should be noted that the form of Eq. 1 is significantly different from that frequently reported for the hydroformylation of light alkenes catalyzed by HRh(CO)(PPh$_3$)$_3$ in homogeneous solution. Under "typical catalytic conditions" (343–393 K, 10–30 atm, and [PPh$_3$]/[Rh] > 100), the rate of aldehyde formation is often positive order in alkene, nearly zero order in H_2 and inverse order in CO and PPh$_3$ [29]. We suggest that the positive order dependences on H_2 and CO seen in this study may reflect the low partial pressures of H_2 and CO used, which result in under-saturation levels of coordinated H and CO. Consistent with this reasoning, we note that positive order kinetics have been reported for alkene hydroformylation carried out at pressures lower than those described as "typical catalytic conditions" [16, 18, 30].

The high n/i ratio observed in the present study for [PPh$_3$]/[Rh] = 15 is also observed in studies conducted with HRh(CO)(PPh$_3$)$_3$ in homogeneous solutions [27]. In contrast, very low n/i ratios have been reported for heterogeneous catalysts [2, 3, 8, 9, 11]. Preference for forming linear versus branched aldehydes has been attributed to the preferred isomerization of HRh(CO)(PPh$_3$)$_2$ to the structure in which both phosphine groups as coordinated in the equatorial plane [27].

The effect of increasing temperature on the rate of n-butanal formation, shown in Fig. 2, may arises from the reversibility of Reaction 7 at higher temperatures. This may occur if the activation energy of the reverse reaction is significantly higher than the forward reaction—therefore the reaction is effectively irreversible at lower temperatures, but becomes reversible when the reverse rate constant becomes sufficiently large at higher temperatures. Stated another way, H_2 desorption becomes important at higher temperatures, similar to CO desorption in carbonylation reactions [31]. If H_2 addition becomes reversible at higher temperatures, the steady state concentration of species **H** decreases, leading to a decrease in the rate of n-butanal formation. This same effect was not observed for isobutanal, perhaps due to its very low rate of formation.

4 Conclusions

Propene hydroformylation reactions catalyzed by PPh$_3$-modified Rh supported on silica producing n- and isobutanal were carried out at different reaction temperatures, propene, CO, and H_2, partial pressures, and PPh3/Rh ratios.

The activation energies and pressure dependences calculated from the data were very similar to those established for homogeneous hydroformylation catalysts. Even the optimum ratio of PPh_3 to Rh was similar to that reported for homogeneous catalysts.

The catalysts produced were very stable and showed 100% selectivity to C_4 aldehydes; no propane or alcohols were detected. The n/i ratio was generally high, ~ 14. Experiments were carried out at low pressures (<3 atm) but a cubic dependence on the total reaction pressure was found (for equimolar reactant mixtures), suggesting that much higher reaction rates could be obtained at only moderately higher pressures.

Due to the similarities between the supported and homogeneous catalysts, we propose that the active species in both systems are in fact identical, with the active homogeneous species formed in situ in the liquid PPh_{3-} phase in the pores of the silica support.

References

1. Cole-Hamilton DJ (2003) Science 299:1702
2. Takahashi N, Kobayashi M (1984) J Catal 85:89
3. Davis ME, Rode E, Taylor D, Hanson BE (1984) J Catal 86:67
4. Naito S, Tanimoto M (1989) J Chem Soc Chem Commun 1403
5. Chung SSC, Pien SI (1992) J Catal 135:618
6. Srinivas G, Chung SSC (1993) J Catal 144:131
7. Zhu H, Ding Y, Yan L, Lu Y, Li C, Bao X, Lin L (2004) Chem Lett 33:630
8. Yan L, Ding YJ, Zhu HJ, Xiong JM, Wang T, Pan ZD, Lin LW (2005) J Mol Catal A Chem 234:1
9. Yan L, Ding Y, Zhu H, Yin H, Jiao G, Zhao D, Lin L (2006) Chin J Catal 27:1
10. Li X, Ding Y, Jiao G, Li J, Lin R, Gong L, Yan L, Zhu H (2009) Appl Catal A 353:266
11. Yan L, Ding YJ, Lin LW, Zhu HJ, Yin HM, Li XM, Lu Y (2009) J Mol Catal A Chem 300:116
12. Lan X, Zhang W, Yan L, Ding Y, Han X, Lin L, Bao X (2009) J Phys Chem C 113:6589
13. Joly JF, Zanier-Szydlowski N, Colin S, Raatz F, Saussey J, Lavalley JC (1991) Catal Today 9:31
14. Xu LQ, Zholobenko VL, Kustov LM, Sachtler WMH (1993) J Mol Catal 83:391
15. Kramer PCJ, Reek JNH, van Leeuwen PWNM (2002) Rhodium phosphite catalysts. In: van Leeuwen PWNM, Claver C (eds) Rhodium catalyzed hydroformylation. Kluwer Academic Publishers, New York, p 36
16. van Leeuwen PWNM, Van Koten G (1995) Homoegeneous catalysis with transition metal complexes. In: Moulijn JA, van Leeuwen PWNM, Van Santen RA (eds) Catalysis. An integrated approach to homogeneous, heterogeneous and industrial catalysis. Elsevier, Amersterdam, p 199
17. Riisager A, Fehrmann R, Haumann M, Gorle BSK, Wasserscheid P (2005) Ind Eng Chem Res 44:9853
18. Bernas A, Maki-Arvela P, Lehtonen J, Salmi T, Murzin DY (2008) Ind Eng Chem Res 47:4317
19. Herman JM, Van den Berg PJ, Scholten JJF (1987) Chem Eng J (Amsterdam, Neth.) 34:123
20. Murzin DY, Bernas A, Salmi T (2010) J Mol Catal A Chem 315:148
21. Yang AC, Garland CW (1957) J Phys Chem 61:1504
22. Basu P, Panayotov D, Yates JT (1988) J Am Chem Soc 110:2074
23. Rice CA, Worley SD, Curtis CW, Guin J, Tarrer AR (1981) J Chem Phys 74:6487
24. Riisager A, Fehrmann R, Flicker S, van Hal R, Haumann M, Wasserscheid P (2005) Angew Chem Int Ed 44:815
25. Evans D, Yagupsky G, Wilkinson G (1968) J Chem Soc A 2660
26. Morris DE, Tinker HB, Chemtech (1972) 554
27. Gerritsen LA, Van Meerkerk A, Vreugdenhil MH, Scholten JJF (1980) J Mol Catal 9:139
28. Mukhopadhyay K, Mandale AB, Chaudari RV (2003) Chem Mater 15:1766
29. van Leeuwen PWNM, Casey CP, Whiteker GT (2002) Phosphines as ligands. In: van Leeuwen PWNM, Claver C (eds) Rhodium catalyzed hydroformylation. Kluwer Academic Publishers, New York, p 63
30. Zakzeski J, Lee HR, Leung YL, Bell AT (2010) Appl Catal A 374:207
31. Celik FE, Kim T, Mlinar AN, Bell AT (2010) J Catal 274:150